ISSN 1063-7729, Astronomy Reports, 2023, Vol. 67, No. 9, pp. 929–937. © The Author(s), 2023. This article is an open access publication.
Russian Text © The Author(s), 2023, published in Astronomicheskii Zhurnal, 2023, Vol. 100, No. 9, pp. 811–819.

Characteristics of Long-Term Spot Activity on Several Late-Spectral-Type Stars

A. V. Kozhevnikova[a],*, I. Yu. Alekseev[b], and V. P. Kozhevnikov[a]

[a] *B.N. Yeltsin Ural Federal University, Yekaterinburg, Russia*
[b] *Crimean Astrophysical Observatory, Nauchny, Russia*
* *e-mail: alla.kozhevnikova@urfu.ru*

Received April 23, 2023; revised May 26, 2023; accepted June 20, 2023

Abstract—We present our analysis of many-year photometry for several dozens of chromospherically active stars that exhibit solar-type activity (from our own observations as well as from data in the literature). Modeling of the distribution of cool photospheric spots, based on the zonal model, was performed, with several hundred models constructed. We find that, for most stars, their spots are located at intermediate and moderate latitudes and that the largest spotted areas can cover from 7 to 58% of the star's surface. We demonstrate that a latitude drift of spots can be suspected for a number of stars, towards the equator as well as towards the pole; however, the rate of this drift is several times lower than for solar spots. For 15 stars, we detected the presence of activity cycles from 3 to 28 years long that reveal themselves in variations of the system's brightness as well as in variations of the total spot coverage of the star. This paper is based on a talk presented at the memorial astrophysical workshop "Novelties in Understanding the Evolution of Binary Stars" dedicated to the 90th birthday of Prof. M.A. Svechnikov.

Keywords: variable stars, stellar activity, star spots

DOI: 10.1134/S1063772923090081

1. INTRODUCTION

Activity processes similar to those observed for the Sun are more and more often detected at other stars, and thus, the topic of solar-stellar physics shows active development [1–3]. Stars of late spectral types with convective envelopes are subject to influence of internal magnetic fields that cause a wide variety of activity manifestations: cool photospheric spots, chromospheric faculae, coronal loops, flares, radiation in ultraviolet, X-ray, and radio ranges [4]. Star spots, the most obvious manifestation of stellar activity, appear at the positions where the magnetic field, strong enough to suppress convective motion in the layers under the photosphere, emerges at the surface, and thus they permit us to obtain some understanding of the star's magnetic field structure. Reviews of properties of active spotted stars and of their role in understanding stellar magnetism can be found, for example, in the papers by Brun and Browning [1], Strassmeier [4], Berdyugina [5] and references therein. Variations of spot parameters with time make it possible to study stellar activity cycles similar to the solar activity cycle as well as to reveal the presence or absence of the so-called active longitudes: regions where photospheric spots are predominately found. Thus, it is very important to obtain information on the spot coverage of stars during long time intervals, covering several decades. Knowledge of the time dynamics of star-spot parameters permits us to improve our understanding of the theory of magnetic fields and promotes development of the unified solar–stellar magnetism theory.

The Sun is the only star where we can study photospheric spots with a high spatial resolution. For other stars, we are limited to only indirect methods in order to obtain information on the presence of star spots or on their physical parameters. The method best suited for a long-term analysis of the behavior of spotted stars is photometry: it permits to obtain long time series of observations for each star, covering many years. The present paper is based on such monitoring performed at the Crimean Astrophysical Observatory and at the Kourovka astronomical observatory of Ural Federal University.

Cool spots reveal themselves photometrically through rotational modulation of the star's brightness with an amplitude from several hundredths to several tenths of a magnitude [5]. Slow changes of the spot configuration cause variations of the light curve from one season to another, reflecting themselves not only in changing shape of the rotational brightness modulation but also in changing general brightness level of the system. Multicolor photometric observations provide most reliable determinations of the temperature and total area of star spots, while estimating the lati-

tude distribution of spots is the most difficult task requiring some a priori assumptions. This problem is widely covered in the literature, different models have been developed (see a review in the book by Gershberg [6]).

This paper presents a generalized analysis of spot coverage for several dozens of chromospherically active stars with spectral types from G to K that belong to the RS CVn and BY Dra types over time scales of tens of years, aimed at detecting long-term variations of photosperic spots and at the search for activity cycles.

2. OBSERVATIONS

Our observations of active variable stars were performed at two observatories: at the astronomical observatory of the Ural Federal University using the 70-cm telescope and a multi-channel photometer that permits simultaneous measurements of the light flux of two stars (the program star and the comparison star) and of the sky background continuously, during the whole night, and at the Crimean Astrophysical Observatory using the 1.25-meter telescope AZT-11. Differential photometry was obtained in the standard *U*, *B*, *V*, *R*, and *I* bands of the Johnson system; standard uncertainties of the determination of the star's brightness and color indices do not exceed $0^{m}.01$. We published details concerning the technique of our observations and observation results in a series of papers [7–9].

For all the program stars, we revealed rotational brightness modulation due to the presence of cool photospheric spots. The shape of the light curve, its amplitude and mean level show changes from one season to another that may be due to slow variations of the spot configuration. An analysis of photometric variations in the *U*, *B*, *V*, *R*, and *I* bands demonstrates that all stars feature reddening at the photometric minimum of rotational modulation, confirming that the modulation is due to cool photometric spots, as it was demonstrated in [6].

To plot long-term light curves for the program stars, we used not only our own observations but also data of photometric observations of the same stars from the literature; a sample of such light curves is presented in Fig 1. The dashed horizontal line shows the level of the historically highest brightness during the whole interval of observations. The vertical bars are brightness variations for each epoch of observations, derived from data on the rotational modulation; dots are episodic observations (if available). The photometric data were taken from [8–28] and from sources referred to in these papers.

3. METHODS USED TO DETERMINE PARAMETERS OF STELLAR PHOTOSPHERIC SPOT COVERAGE

We modeled spot coverage of photospheres using our own observations of the star as well as all photometric data available in the literature. In this modeling, we used the zonal spot coverage model developed in the Crimean Astrophysical Observatory [29]. In variance with the traditional scheme that considers one or two spots on a star, our model considers general characteristics of the spotted region as a whole and describes the photometric behavior of spotted stars using the concept of numerous small spots located in two latitude belts, similar to royal latitudes on the Sun. Unlike the previous version [30], our model now permits to consider simultaneous presence of two active longitudes on the star where spots are formed. It was demonstrated in several studies [4, 5, 31] that simultaneous presence of two active longitudes was rather often observed for spotted stars of all spectral types and luminosities, including the Sun. It is important that modeling in the frame of this scheme considers the long-term behavior of the star during previous decades, permitting to estimate the star's highest brightness for the whole time interval of its photometric observations and to consider this value, with a high probability, as the star's brightness in a state free of spots.

The whole system of spotted areas on the star was represented with two spotted belts, symmetrical with respect to the equator. They occupy regions with latitudes from $\pm\varphi_0$ to $\pm(\varphi_0 + \Delta\varphi)$, with the density of spot coverage $f(l)$ that varies along the longitude from unity at the star's primary brightness minimum to certain vales f_1 and f_2, respectively in the seasonal maximum and secondary minimum, so that $0 < f_1 < f_2 < 1$. In the process of modeling, we use three extreme points of the light curve for each season: the local maximum and the primary and secondary brightness minima (respectively ΔV_{max}, ΔV_1, and ΔV_2), referred to the maximum brightness of the system during the whole time interval of observations, V_{max} (column 3 in Table 1 and horizontal dashed lines in Fig. 1). Our computations use observations in the *B*, *V*, *R*, and *I* bands of the Johnson system, permitting us not only to correctly separate the geometric effect of the spot coverage from the temperature one but also to consider latitude effects in the spot distribution [26]. We did not use data in the *U* photometric band: for all types of spotted stars, the light in this band is distorted with the chromospheric activity. Assumptions concerning the energy distribution in the spectrum of the cool spot play in important role in the computations. We assume that this energy has the same distribution as in the spectrum of a star of a later spectral type. Other important input model parameters are the inclination *i* of the star's rotation axis, its photospheric temperature T_{phot}, and surface gravity log *g* (needed for the

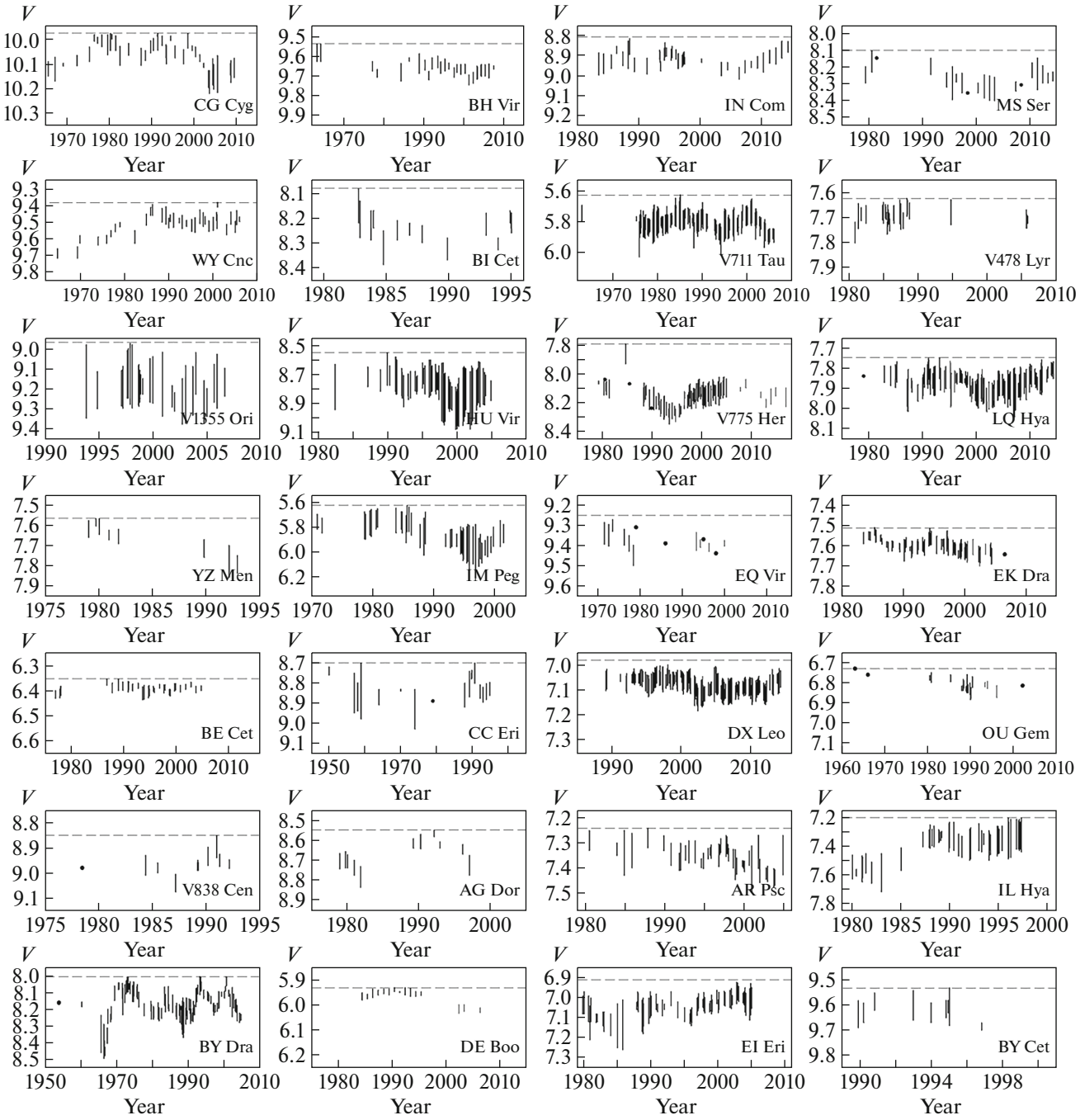

Fig. 1. Long-term brightness diagrams for stars with chromospheric activity. A vertical bar shows the range of the star's brightness variation from minimum to maximum for a given epoch of observations. Solid curves show activity cycles.

choice of limb darkening coefficients). These parameters were taken from the literature [10–28].

The desired characteristics in our model are distances of the spotted belts from the equator $\pm\varphi_0$, the width of these belts $\Delta\varphi$, filling factors f_1 and f_2, contrast of spots in one of the bands (for example, β_V). From these parameters, we determine the mean latitude of spots $\langle\varphi\rangle = \varphi_0 + \Delta\varphi/2$, the area of spots as a fraction of the whole surface of the star $S = (2\pi)^{-1} \times (\sin(j_0 + Dj) - \sin j_0)\int f(l)\mathrm{d}l$, where the integral over longitude is taken from 0 to 2π, and the temperature difference ΔT between the quiet photosphere and spots.

Table 2 presents determination errors of spotted area parameters, dependent upon input model param-

Table 1. Main spot parameters for program stars

Star	Sp	V_{max}, mag	No. of epochs	ΔT_{spot}, K	$\langle\varphi\rangle$, deg	S_{max}, %	$\delta\varphi$, deg/year	R ($\langle\varphi\rangle$, S)	P_{cyc}, years
LQ Hya	K1V	7.75	166	800	35–51	29.5	–0.9...–1.7	—	18, 11.2, 15, 6.75, 5.2
EQ Vir	K6V	9.25	15	960	2.2–5.7	14.6	—	0.74	—
EK Dra	G1V	7.48	82	2300	46–64	23.6	–1.6...–2.0	–0.73	27, 12, 9.2, 6.5, 4.5
DX Leo	K0V	6.98	137	1480	38–54	17.0	–2.2...–2.6	–0.56	14, 3.2
OU Gem	K3V + K5V	6.73	24	1850	18–20	16.1	—	—	
V833 Tau	K5V	7.88	67	950	20–29	58.6	0.8	0.75	20, 6.4
BY Dra	K7V + K8V	8.00	125	950	2.7–21.5	56.0	1.2...1.6	0.95	13.7, 9, 2.7
BE Cet	G2V	6.352	33	1570	52.6–55.2	11.4	—	—	6.7, 9.1
CC Eri	K7V + M0V	8.70	17	830	3.8–17.0	35.1	—	0.74	—
V838 Cen	K1V + K1V	8.85	11	970	5.8–12.4	36.6	—	0.87	—
AG Dor	K1V + K5V	8.55	11	1300	1.2–7.3	21.8	—	0.90	—
DE Boo	K2V	5.93	15	1200	0.4–2.5	7.1	0.2	0.92	—
CG Cyg	G9V + K3V	9.98	39	2100	0–7	18	0.8	0.93	17
BH Vir	G0V + G5V	9.54	26	2300	32–34	26	—	—	23
WY Cnc	G5V + M2V	9.38	37	1700	1–7	21	–0.2	0.96	—
BI Cet	G6IV/V + G6V	8.08	14	2250	26–52	47	—	—	—
IN Com	G5III/IV	8.81	40	600	39–55	22	0.6	–0.50	7; 20
MS Ser	K2IV + G8V	8.11	19	1300	23–49	24	–2.5	–0.76	—
V711 Tau	K1IV + G5V	5.63	255	1300	30–46	41	–1.9	—	16.5; 5.5
V478 Lyr	G8V + M3V	7.625	25	1850	18–27	10	—	–0.65	6.7
IL Hya	K1III/IV + G0V	7.20	48	1500	40–58	43	—	–0.54	13
EI Eri	G5IV	6.92	61	1200	40–57	36	–1.0...–2.9	—	16
BY Cet	G7V + K5V	8.08	9	2100	2–4	12	—	—	—
AR Psc	K1IV + G5/6V	7.24	39	600	7–17	40	—	0.73	—
V1355 Ori	K2IV/V + G8V	8.97	28	1500	40–56	34	—	–	—
HU Vir	K1IV	8.55	58	1650	6–12	27	0.8	0.78	6
YZ Men	K1III	7.52	8	900	23–27	46	—	—	—
IM Peg	K2III	5.55	43	1500	6–13	29	1.1...–0.9	0.89	10.1; 28.2

eters. Thus, errors of the parameters φ_0 and $\Delta\varphi$ can reach 10°, being mainly determined with uncertainties in the estimates of the angle i and of the coefficient dB/dV. Errors of the filling parameters f_1 and f_2 depend mainly on uncertainties in the extreme points of the light curve and of the angle i; as a rule, they do not exceed 0.04. The spotted area S is estimated with an uncertainty not worse than 10%. The error in the determination of spot temperature is due to uncertainty in the coefficients dB/dV, dR/dV, dI/dV, which are determined from multicolor photometric observations; the uncertainty of 0.01–0.05 in the photometry gives the error of 50–80 K in the temperature.

Some of our program stars are binaries; like in most other studies, we assumed that the spotted star was the primary component of the system [19, 33–37]. As it was demonstrated, for example, in [38], the temperature and luminosity of the secondary components of the studied short-period RS CVn systems are lower than for the primaries by an amount that large that the activity of the secondary component is not able to produce the observed photometric effect. The luminosity difference of the components is still higher for classical RS CVn systems. Thus, when modeling the spot coverage, we primarily considered the dilution effect from the secondary, i.e., subtracted its contribution from the combined brightness of the star.

The most successful current technique for studies of stellar surface inhomogeneities is that of Doppler mapping, based on studying small deformations of photospheric line profiles in the presence of surface inhomogeneities. However, such studies require a high signal-to-noise ratio and a good spectroscopic resolution within a line and thus can be applied by far not to all stars. By now, only some 80 objects of several hundred known spotted stars have been studies using the

Table 2. Relation between determination errors of spotted-area parameters and uncertainties of model input parameters

Parameter	±	φ_0, deg	$\Delta\varphi$, deg	f_1, f_2	β_V	ΔT, K	S, %
T_{phot}, K	250	1	2	0.01	0.01	70	1.5
log g	0.5	<1	<0.1	<0.01	<0.01	5	<0.1
V_{max}, mag	0.01	1	1.5	0.04	<0.01	10	1
ι, deg	10	5	6	0.02	0.05	80	6
dB/dV	0.05	6	10	0.02	0.04	80	10
dR/dV	0.02	3	5	0.01	0.04	60	7
dI/dV	0.01	2	4	0.01	0.03	50	3

Doppler mapping method. In our list, such observations are available, at least for a single season, for 11 objects (IM Peg, II Peg, V711 Tau, LQ Hya, EK Dra, AG Dor, IN Com, V1355 Ori, IL Hya, EI Eri, HU Vir). Usually their results do not contradict our computations of the spotted area but often predict warmer spots, possibly because of the method's lower sensitivity to lower spot temperatures. Note that this method can predict the presence of high-latitude spots for most stars, while our methods tend to predict low- and intermediate-latitude spots. Alekseev and Kozlova [39] plotted synthetic light curves in the *BVRI* bands for published Doppler maps of LQ Hya and demonstrated that, while the extreme light-curve points were reproduced with an accuracy worse than $0^m.03$, the dB/dV, dR/dV, and dI/dV coefficients they derived were reproduced with an accu-

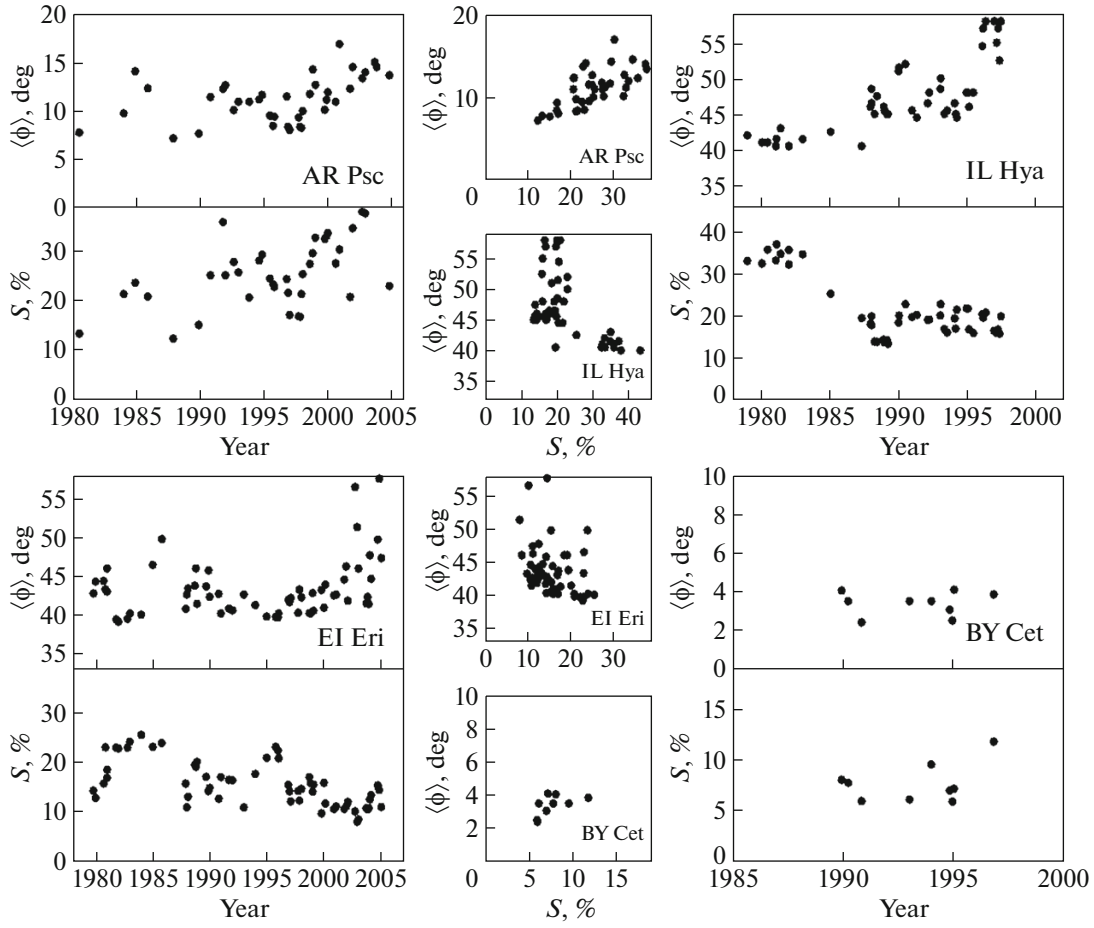

Fig. 2. Examples of variations of the mean latitude of the spotted belt in the northern hemisphere and of the total area S covered with spots versus time, for four short-period RS CVn systems: AR Psc, IL Hya, EI Eri, and BY Cet. The middle panel shows the relation between the mean latitude of spotted areas, for all epochs of observations, and total area of spots.

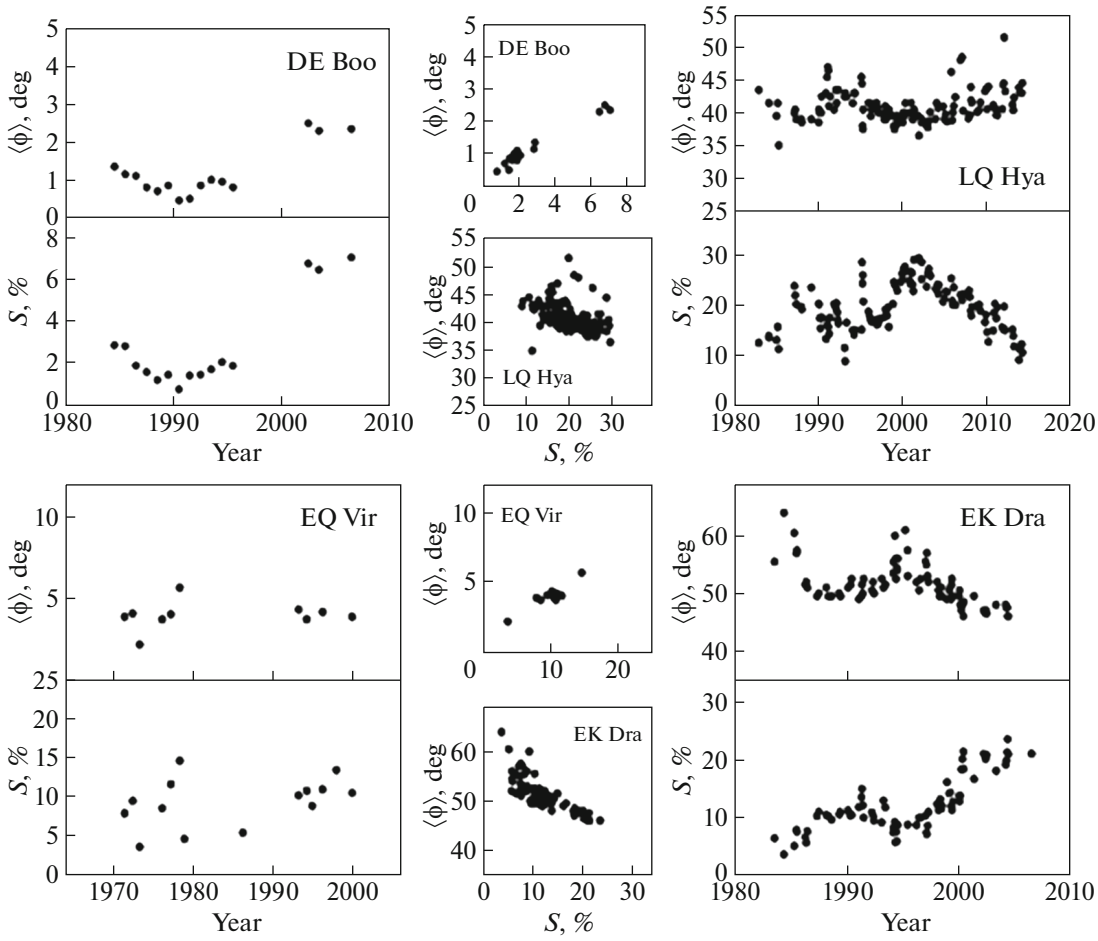

Fig. 3. Examples of variations of the mean latitude of the spotted belt in the northern hemisphere and of the total area S covered with spots versus time, for four BY Dra stars: DE Boo, LQ Hya, EQ Vir и EK Dra. The middle panel shows the relation between the mean latitude of spotted areas, for all epochs of observations, and total area of spots.

racy worse than 0.10. Thus, Doppler mapping is often unable to produce good agreement with photometric observations.

Unfortunately, many-year regular Doppler observations are available only for a handful of stars. In our sample, these are 4 stars only: IM Peg (regular observations started in 1996 [40]); II Peg (mapping started in 1992 [41]); V711 Tau (since 1981 [42]); and LQ Hya (studied since 1991 [43]). For these variables, we are able to follow long-term variations of areas and mean latitudes of the spotted regions due to activity cycles of the stars. Note that the cycle durations are already known from photometric observations and coincide with those we found.

4. RESULTS AND CONCLUSIONS

Our modeling of spot coverage for twenty-eight chromospherically active stars of the RS CVn and BY Dra types over time intervals from 11 to 52 years demonstrates that photometric behavior of all the program stars is successfully described with the zonal model of spots that permits to consider simultaneous presence of spots at two active longitudes of the star. The parameters we determined for spotted areas of all the stars are collected in Table 1. For each star, the Table presents its spectral type Sp; its historically brightest magnitude V_{max}; the number of epochs we analyzed; the temperature difference between spots and unspotted photosphere ΔT_{spot}; the variation range of the mean spotted-belt latitude $\langle\varphi\rangle$ for the star's northern hemisphere; the historically largest spotted area of the star S_{max}, in percents of the star's total surface area; the rate of the latitude drift of the spots $\delta\varphi$; the correlation coefficients $R(\langle\varphi\rangle, S)$, provided that the spot latitudes were found dependent on their area; and the activity cycles P_{cyc}.

Our modeling demonstrated that the mean latitudes of spotted areas $\langle\varphi\rangle$ were between 0° and 64°. For some stars, we found data on their high-latitude activity: for example, for the star IL Hya, the upper boundary of spots reached 81° in 1996. For nine stars, two spotted belts symmetrical with respect to the equator

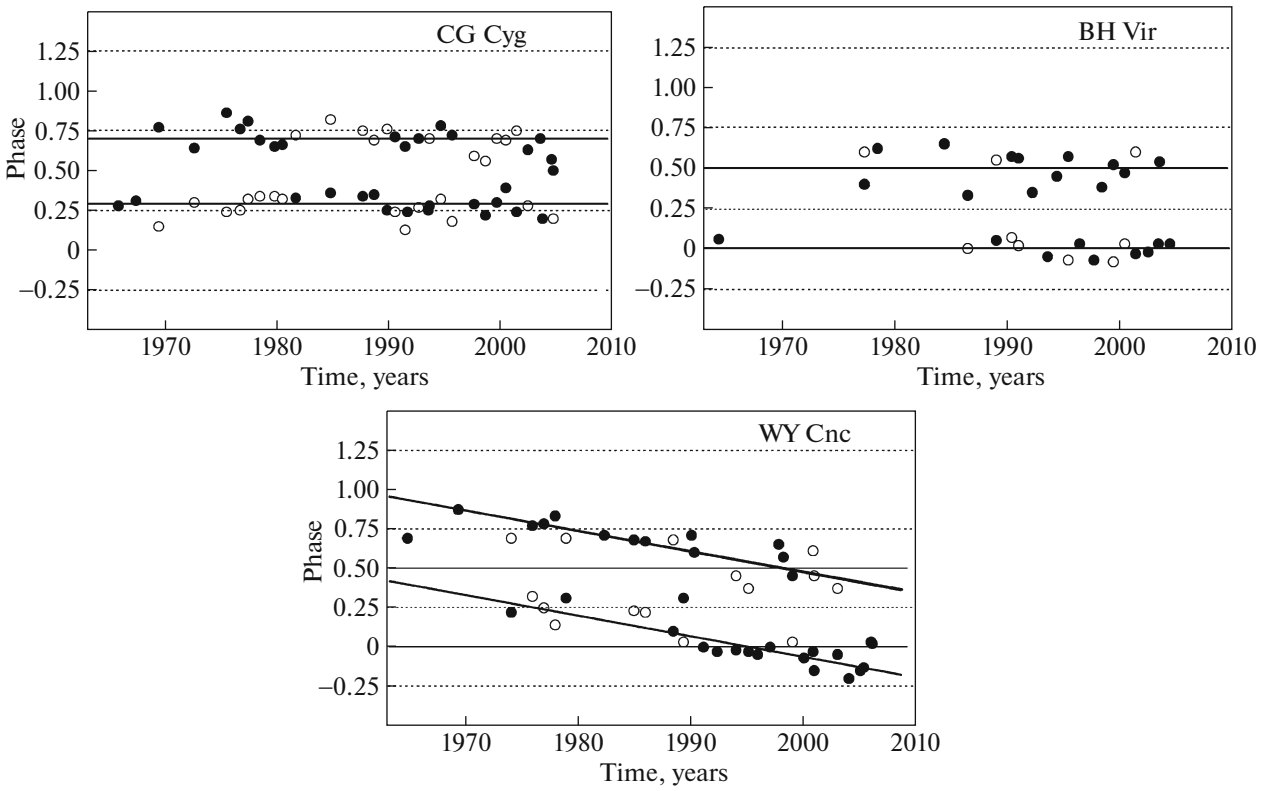

Fig. 4. Variations of the position of maximum spot coverage longitudes with time for BH Vir, CG Cyg. and WY Cnc. Straight lines are mean positions of active longitudes. The filled symbol corresponds to the dominating mean longitude and the open symbol, to the secondary longitude.

merge into a single belt (the distance from the equator to the spotted belts being $\varphi_0 = 0°$ for all the epochs). These are three systems consisting of dwarf components: CG Cyg, WY Cnc, BY Cet; two subgiant components: HU Vir and IM Peg; and the BY Dra-type dwarfs: CC Eri, BY Dra, EQ Vir, and AG Dor. A half of the stars show a latitude drift of spots, towards the equator as well as towards the pole for different time intervals. This behavior can be considered a rough analog of the solar Maunder "butterfly" diagram, as it was first suggested by Livshits et al. [44]. The absolute value of the suggested latitude spot drift rate is, as a rule, lower than the corresponding value for solar spots by a factor of 2–3, but it agrees with estimates for several dwarf stars of the G and K spectral types [45]. The spotted area S varies between 7 and 58% of the star's total surface for different epochs of observations. Examples of variations of spot parameters with time, found in the frame of the zonal model, and dependences of the mean latitude of spotted regions on their area are shown in Fig. 2 (for RS CVn stars) and Fig. 3 (for BY Dra stars).

Eighteen stars show a correlation or an anti-correlation between the latitude of the spotted regions and their area. For four systems featuring an increase of the area of spots during the increase of their latitude for the whole studied time interval (32–50 years), the correlation coefficient $R(\langle\varphi\rangle, S)$ is very high: CG Cyg ($R = 0.93$), WY Cnc ($R = 0.96$), IM Peg ($R = 0.89$), BY Dra ($R = 0.95$). An increase of the area with decreasing latitude, similar to the pattern known for sunspots, is detected for six systems, but the correlation coefficients are lower: MS Ser ($R = -0.76$), IN Com ($R = -0.50$), V478 Lyr ($R = -0.65$) и IL Hya ($R = -0.54$), EK Dra ($R = -0.73$), DX Leo ($R = -0.56$). Thus, the correlation is stronger for those stars that show increasing spot area during the decrease of their latitude in the whole studied time interval.

We demonstrated for several stars that their spots were observed at two preferred, so-called active, longitudes, i.e., the heaviets-spotted regions are located at the preferred active longitudes. For some of the stars, these regions are fixed during the whole studied time interval and separated approximately by 180° (see Fig. 4). The pattern observed for other stars is like that for WY Cnc: maxima of the spot distribution drift with time but remain separated by approximately a half of the orbital period. For all the systems, from time to time, activity switches from one longitude to the other one: this is the so-called "flip-flop" effect first detected for stars of the FK Com type and later, for RS CVn systems [46]. The presence of two preferred active longitudes can indicate a non-symmetrical character of stellar magnetic fields.

Periodic variations of photometric brightness and spot latitudes suggest the presence of activity cycles for 15 stars, with cycle duration from 2.7 to 28 years: CG Cyg, BH Vir, AR Psc, V478 Lyr, IN Com, V 711 Tau, EI Eri, Il Hya, AD Leo, EV Lac, FF And, V1005 Ori, GT Peg, and DT Vir. The activity cycles reveal themselves in synchronous variations of the area and latitude of spots with time as well as in variations of the star's total photometric brightness. The derived cycle lengths agree with the earlier known cycles of these active stars derived from variations of their optical brightness as well as from the analysis of their chromospheric and X-ray radiation: from several years to dozens of years [47–49]. We found no qualitative difference of the long-term spot coverage variations between RS CVn systems and BY Dra dwarfs or between binary and single stars.

FUNDING

Thus study was financially supported by the Ministry of Science and Higher Education of Russian Federation, theme FEUZ-2023-0019.

CONFLICT OF INTEREST

The authors declare that they have no conflicts of interest.

OPEN ACCESS

REFERENCES

1. A. S. Brun and M. K. Browning, Liv. Rev. Sol. Phys. **14**, 133 (2017).
2. M. M. Katsova, L. L. Kitchatinov, D. Moss, K. Oláh, and D. D. Sokoloff, Astron. Rep. **62**, 513 (2018).
3. V. N. Obridko, M. M. Katsova, and D. D. Sokoloff, Mon. Not. R. Astron. Soc. **516**, 1251 (2022).
4. K. G. Strassmeier, Astron. Astrophys. Rev. **17**, 308 (2009).
5. S. V. Berdyugina, Liv. Rev. Solar Phys. **2**, 1 (2005).
6. R. E. Gershberg, *Solar-Type Activity in Main-Sequence Stars* (AstroPrint, Odessa, 2002; Springer, Berlin, 2005).
7. A. V. Kozhevnikova, V. P. Kozhevnikov, I. Yu. Alekseev, I. A. Yushkov, and A. A. Dorogov, Astron. Rep. **56**, 281 (2012).
8. A. V. Kozhevnikova and I. Yu. Alekseev, Astron. Rep. **59**, 937 (2015).
9. I. Yu. Alekseev and A. V. Kozhevnikova, Astron. Rep. **62**, 396 (2018).
10. M. Zeilik, S. Gordon, E. Juderlund, et al., Astrophys. J. **421**, 303 (1994).
11. S. A. Naftilan and E. F. Milone, Astron. J. **84**, 1218 (1979).
12. C. Lazaro and M. J. Arevalo, Astron. J. **113**, 2283 (1997).
13. M. Afsar, P. A. Heckert, and C. Ibanoglu, Astron. Astrophys. **420**, 595 (2004).
14. S. Messina and E. F. Guinan, Astron. Astrophys. **393**, 225 (2002).
15. S. Messina and E. F. Guinan, Astron. Astrophys. **409**, 1017 (2003).
16. S. P. Jarvinen, S. V. Berdyugina, and K. G. Strassmeier, Astron. Astrophys. **440**, 735 (2005).
17. K. G. Strassmeier and J. B. Rice, Astron. Astrophys. **330**, 685 (1998).
18. J. D. Dorren, M. Güdel, and E. F. Guinan, Astrophys. J. **448**, 431 (1995).
19. G. Cutispoto, S. Messina, and M. Rodonó, Astron. Astrophys. **400**, 659 (2003).
20. A. Udalski and E. H. Geyer, Inform. Bull. Var. Stars **2525**, 1 (1984).
21. A. Udalski and E. H. Geyer, Inform. Bull. Var. Stars **2691**, 1 (1985).
22. G. Cutispoto, Astron. Astrophys. Suppl. Ser. **131**, 321 (1998).
23. S. V. Berdyugina, J. Pelt, and I. Tuominen, Astron. Astrophys. **394**, 505 (2002).
24. S. L. Baliunas, R. A. Donahue, W. H. Soon, et al., Astrophys. J. **438**, 269 (1995).
25. S. Messina, E. F. Guinan, A. F. Lanza, and C. Ambruster, Astron. Astrophys. **347**, 249 (1999).
26. G. W. Lockwood, B. A. Skiff, G. W. Henry, S. M. Henry, R. R. Radick, et al., Astrophys. J. Suppl. Ser. **171**, 260 (2007).
27. T. Lloyd-Evans and M. C. J. Koen, South. Afr. Astron. Obs. Circ. **11**, 21 (1987).
28. G. Cutispoto, S. Messina, and M. Rodonó, Astron. Astrophys. **367**, 810 (2001).
29. I. Yu. Alekseev, Izv. Krymsk. Astrofiz. Observ. **104**, 272 (2008).
30. I. Yu. Alekseev and R. E. Gershberg, Astron. Rep. **40**, 538 (1996).
31. K. Olah, Astrophys. Space Sci. **304**, 145 (2006).
32. I. Yu. Alekseev, *Low-Mass Spotted Stars* (AstroPrint, Odessa, 2001) [in Russian].
33. D. P. Kjurkchieva, D. V. Marchev, and W. Ogloza, Astron. Astrophys. **400**, 623 (2003).
34. D. P. Kjurkchieva, D. V. Marchev, P. A. Heckert, and C. A. Shower, Astron. Astrophys. **424**, 993 (2004).
35. M. Zeilik, M. Ledlow, M. Rhodes, et al., Astrophys. J. **354**, 352 (1990).

36. D. Kjurkchieva, D. Marchev, and W. Ogloza, Astron. Astrophys. **415**, 231 (2004).
37. E. Budding and M. Zeilik, Astrophys. J. **319**, 827 (1987).
38. P. Vivekananda Rao, M. B. R. Sarma, and B. V. N. S. Praksa Rao, J. Astrophys. Astron. **12**, 225 (1991).
39. I. Yu. Alekseev and O. V. Kozlova, Astron. Astrophys. **396**, 203 (2003).
40. S. V. Berdyugina, A. V. Berdyugin, I. V. Ilyin, and I. Tuominen, Astron. Astrophys. **360**, 272 (2000).
41. S. V. Berdyugina, I. V. Berdyugin, I. V. Ilyin, and I. Tuominen, Astron. Astrophys. **350**, 626 (1999).
42. S. S. Vogt, A. Hatzes, A. Misch, and M. Kürster, Astrophys. J. Suppl. **121**, 547 (1999).
43. K. G. Strassmeier, J. B. Rice, W. Wehlau, et al., Astron. Astrophys. **268**, 671 (1993).
44. M. A. Livshits, I. Yu. Alekseev, and M. M. Katsova, Astron. Rep. **47**, 562 (2003).
45. M. M. Katsova, M. A. Livshits, and G. Belvedere, Solar Phys. **216**, 353 (2003).
46. S. V. Berdyugina and I. Tuominen, Astron. Astrophys. **336**, 25 (1998).
47. E. A. Bruevich, M. M. Katsova, and D. D. Sokolov, Astron. Rep. **45**, 718 (2001).
48. D. S. Hall, Astrophys. J. **380**, L85 (1991).
49. K. Oláh, Z. Kolláth, and K. G. Strassmeier, Astron. Astrophys. **356**, 643 (2000).